

Determining the Three-Dimensional Phase Center of an Antenna

Ying Chen¹ and Rodney G. Vaughan¹

¹School of Engineering Science, Simon Fraser University, Burnaby, BC, Canada, V5A1S6
yca180@sfu.ca and rodney_vaughan@sfu.ca

Abstract

A method for determining the best-fit phase center of an antenna is presented. Electrically small antennas with simple patterns and linear polarizations can have well-defined phase centers, but this is not the case for antennas with more sophisticated patterns, including those with circular polarization. In general, the phase center is sensitive to the angular range of interest, the weighting over that angular range, and of course the frequency. The formulation is developed here for finding the physical location on an antenna which corresponds to a minimum variance for an antenna's angularly weighed phase pattern. Examples using measurements of specialist precision GPS antennas are used to give a feel for the results. A brute-force search is used, but the relatively small nature of the problem means that the solution is quick when using a standard personal computer.

1. Introduction

The phase center of an antenna is the point from which the radiation spreads spherically, with the phase being equal at any point of the sphere. The phase center is normally not uniquely defined, in the sense that it depends on the details of the range of antenna parameters, including basic variables such as the frequency, the angles of interest within the pattern, and the relative weightings of these. Narrowband antennas are often taken to mean that their parameters are independent of frequency, although this is seldom the case, especially with phase behavior.

The example presented in this paper is for GPS applications, where inaccuracy in the phase center estimate causes significant errors for positioning services [1]. Several different approaches for general phase center determination have been put forward [2]–[6]. The three-point approach [2], [3] is the simplest method. But restricting the angular range to only three samples means a single pattern cut which is minimally sampled. Using more data from the cut, a modified method which applies a least squares model to fit all the data to the phase front is presented in [4], [5]. Furthermore, weighting coefficients can be introduced into the least squares fit method to get the phase center [6]. The power pattern of the antenna is usually chosen for finding the weighting coefficients. However, the above methods are only for two-dimensional or single pattern cut. As far as the authors aware, there is no three-dimensional treatment of this problem. The three-dimensional treatment is critical for high accuracy applications such as navigation antennas.

The contribution of this paper is a new approach for determining the three-dimensional phase center. From the raw measured data, we get an updated phase pattern by perturbing the origin of the pattern of the antenna-under-test (AUT). The variance of the new phase pattern is computed using an angular probability density function (pdf). In this paper, two types of pdfs are adopted: the normalized power pattern and a uniform (omni-directional) distribution. The three-dimensional phase center \mathbf{d} (Δx , Δy , Δz) is determined through minimizing the variance of the phase pattern. The application is demonstrated using the right-hand circularly polarized (RHCP) pattern of a GPS antenna designed for precision location.

2. Formulation

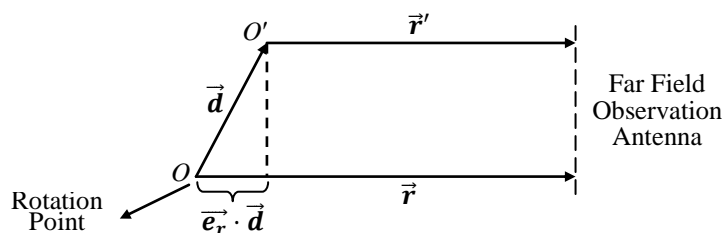


Fig. 1. Coordinate systems of the radiation pattern measurement geometry and relative movement.

Fig. 1 depicts the coordinate system notation. The origin O is the rotation center in the measurement, and a translation \mathbf{d} provides the perturbed coordinate origin O' . With time harmonic dependence $e^{j\omega t}$ understood, the antenna's electric field radiation pattern is denoted as

$$\mathbf{E}(\theta, \varphi) = \vec{\mathbf{u}}E_u(\theta, \varphi)e^{j\phi(\theta, \varphi)} \quad (1)$$

where $\vec{\mathbf{u}}$, $E_u(\theta, \varphi)$ and $\phi(\theta, \varphi)$ are the polarization vector, the far field amplitude pattern and phase pattern, respectively. The observation antenna is assumed to be in the far-field, meaning that the position vectors ($\vec{\mathbf{r}}$ and $\vec{\mathbf{r}}'$) are taken as parallel, and that the zenith and azimuth angles in these two coordinate systems are equivalent, i.e., $\theta = \theta'$ and $\varphi = \varphi'$. The pattern in the new coordinate system can be written as

$$\mathbf{E}'(\theta', \varphi') = \mathbf{E}'(\theta, \varphi) = \vec{\mathbf{u}}E_u(\theta, \varphi)e^{j\phi(\theta, \varphi)}e^{-jk\vec{\mathbf{e}}_r \cdot \vec{\mathbf{d}}} = \vec{\mathbf{u}}E_u(\theta, \varphi)e^{j\Phi(\theta, \varphi)} \quad (2)$$

$$\Phi(\theta, \varphi) = \phi(\theta, \varphi) - k\vec{\mathbf{e}}_r \cdot \vec{\mathbf{d}}$$

and $\vec{\mathbf{e}}_r$ is the unit position vector with k the wave number. $\Phi(\theta, \varphi)$ is the new phase pattern in the new coordinate system. With

$$\vec{\mathbf{d}} = \Delta x\vec{\mathbf{e}}_x + \Delta y\vec{\mathbf{e}}_y + \Delta z\vec{\mathbf{e}}_z, \quad \vec{\mathbf{e}}_r = \sin\theta\cos\varphi\vec{\mathbf{e}}_x + \sin\theta\sin\varphi\vec{\mathbf{e}}_y + \cos\theta\vec{\mathbf{e}}_z, \quad (3)$$

the term $\Phi(\theta, \varphi)$ in (2) becomes

$$\Phi(\theta, \varphi) = \phi(\theta, \varphi) - k\vec{\mathbf{e}}_r \cdot \vec{\mathbf{d}} = \phi(\theta, \varphi) - k(\Delta x\sin\theta\cos\varphi + \Delta y\sin\theta\sin\varphi + \Delta z\cos\theta). \quad (4)$$

The ideal phase center corresponds to when the phase pattern does not change under rotation around this point, which means the variance of the phase pattern is zero. By minimizing the variance of the new phase pattern, the best fit phase center is found. An angular *probability density function* (pdf) is introduced,

$$p_{\theta, \varphi}(\theta, \varphi) = \frac{P(\theta, \varphi)}{\int_{\Omega_0} P(\theta, \varphi)d\Omega} \quad (5)$$

where $P(\theta, \varphi)$ is, for example, the co-polarized far field power pattern of the antenna and its normalized form is $p_{\theta, \varphi}(\theta, \varphi)$. This pdf emphasizes the angles where the energy is high, and de-emphasizes the angles where the energy is low. The observation solid angle Ω_0 could be the full sphere (4π), or could be for partial coverage. The variance of $\Phi(\theta, \varphi)$ is

$$\text{Var}[\Phi(\theta, \varphi)] = \langle \Phi(\theta, \varphi)^2 \rangle - \langle \Phi(\theta, \varphi) \rangle^2 \quad (6)$$

where $\langle \Phi(\theta, \varphi) \rangle = \int_{\Omega_0} p_{\theta, \varphi}(\theta, \varphi)\Phi(\theta, \varphi)d\Omega$ and $\langle \Phi(\theta, \varphi)^2 \rangle = \int_{\Omega_0} p_{\theta, \varphi}(\theta, \varphi)\Phi(\theta, \varphi)^2d\Omega$

In perturbing the origin (phase center), some simple patterns feature a single minimum of this variance, but in general the variance has local minima. Consequently an exhaustive search is used to find the optimum. Although slow for large problems, the exhaustive search is the most accurate and is suitable for solving this relatively a small problem. (There are only three variables here.) For frequency variations, the same approach can be used, but using a pdf for the different frequency patterns.

3. Application to a GPS Antenna

From the transmitter's point of view, complex vector for right-hand circularly polarized (RHCP) is given by [7]:

$$\vec{\mathbf{e}}_{\text{RHCP}} = (\vec{\mathbf{e}}_\theta - j\vec{\mathbf{e}}_\varphi)e^{-j\varphi}/\sqrt{2} \quad (7)$$

where $\vec{\mathbf{e}}_\theta$ and $\vec{\mathbf{e}}_\varphi$ are the usual linear polarization (raw data form) vectors. The E-field radiation pattern of an antenna can be expressed as

$$\mathbf{E}(\theta, \varphi) = \vec{\mathbf{e}}_\theta E_\theta e^{j\phi_\theta} + \vec{\mathbf{e}}_\varphi E_\varphi e^{j\phi_\varphi} \quad (8)$$

where E_θ and E_φ are the amplitudes along the $\vec{\mathbf{e}}_\theta$ and $\vec{\mathbf{e}}_\varphi$ directions, respectively; and ϕ_θ and ϕ_φ are their corresponding phases. $\mathbf{E}(\theta, \varphi)$ can be transformed into its RHCP component by:

$$E_{\text{RHCP}}(\theta, \varphi) = \vec{\mathbf{e}}_{\text{RHCP}}^* \cdot \mathbf{E}(\theta, \varphi) = \frac{(E_\theta \cos \phi_\theta - E_\varphi \sin \phi_\varphi) + j(E_\theta \sin \phi_\theta + E_\varphi \cos \phi_\varphi)}{\sqrt{2}} e^{j\varphi} \quad (9)$$

and the phase of the RHCP component is

$$\Phi_{\text{RHCP}} = \tan^{-1} \frac{E_{\theta} \sin \phi_{\theta} + E_{\varphi} \cos \phi_{\varphi}}{E_{\theta} \cos \phi_{\theta} - E_{\varphi} \sin \phi_{\varphi}} + \varphi \quad (10)$$

Fig. 2 (a) shows the power patterns of the RHCP component on three selected cuts ($\varphi = 0^\circ, 45^\circ$ and 90°). The power patterns are exactly the same (to within the linewidth of the graph) on the different cuts. Fig. 2 (b) shows the phase patterns of the RHCP component on the different cuts. As can be seen, the phase variation is very low for $\theta \in (-50^\circ, 50^\circ)$; however it drops quickly (i.e., varies much more) as θ increases from 50° to 90° . In this example, the angular ranges for calculation are selected as $-50^\circ < \theta < 50^\circ$, and $-90^\circ < \theta < 90^\circ$, respectively.

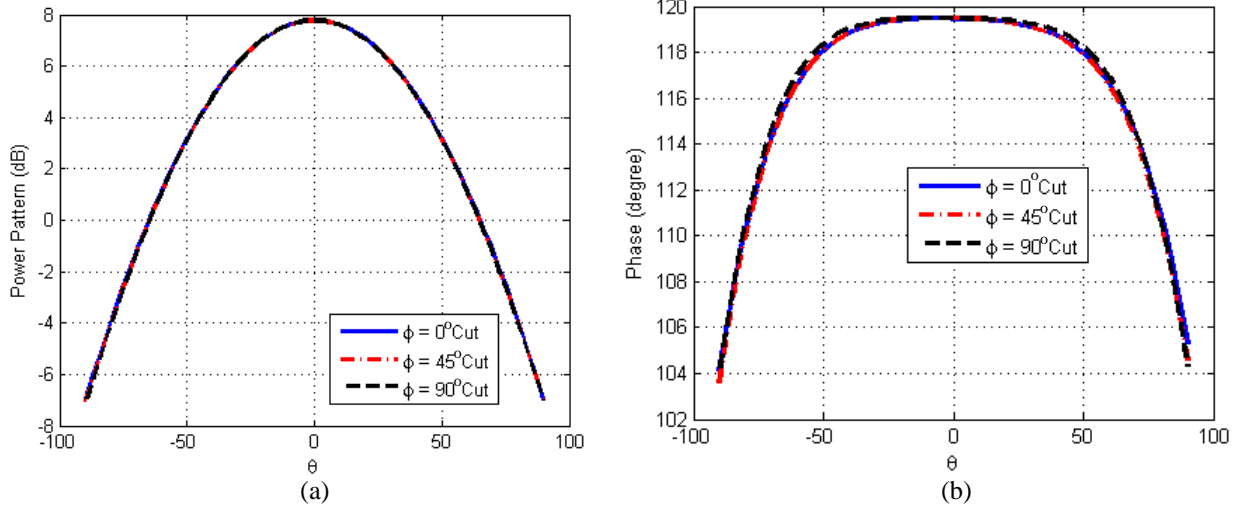


Fig. 2. Measured RHCP patterns on three different cuts ($\varphi = 0^\circ, 45^\circ, 90^\circ$). (a) Power pattern. (b) Phase pattern.

Table I shows the 3D phase centers and their variances for the angular ranges of $-90^\circ < \theta < 90^\circ$, using the two pdfs for a test antenna. In the discussion below, “weighting” refers to using the normalized power pattern for the pdf, and non-weighting refers to the uniform distribution over the angular range. The variance of the original phase pattern (with the power pattern as its pdf) is also listed for comparison, where the *original pattern* corresponds to have the phase center at a referenced location. The variances using weighting and no weighting are 2.109 and 0.981, respectively; and for context, the variance of the original phase pattern is 6.710. To get a feel for the mechanisms behind the reduced variance, Fig. 3 plots the phase patterns on two cuts ($\varphi = 0^\circ$ and $\varphi = 90^\circ$). Table II and Fig. 4 show similar results for the solid angle $-50^\circ < \theta < 50^\circ$. Here, the variance of the original phase pattern is already relatively small (0.087). The new phase patterns have variances of 0.005 and 0.003, respectively.

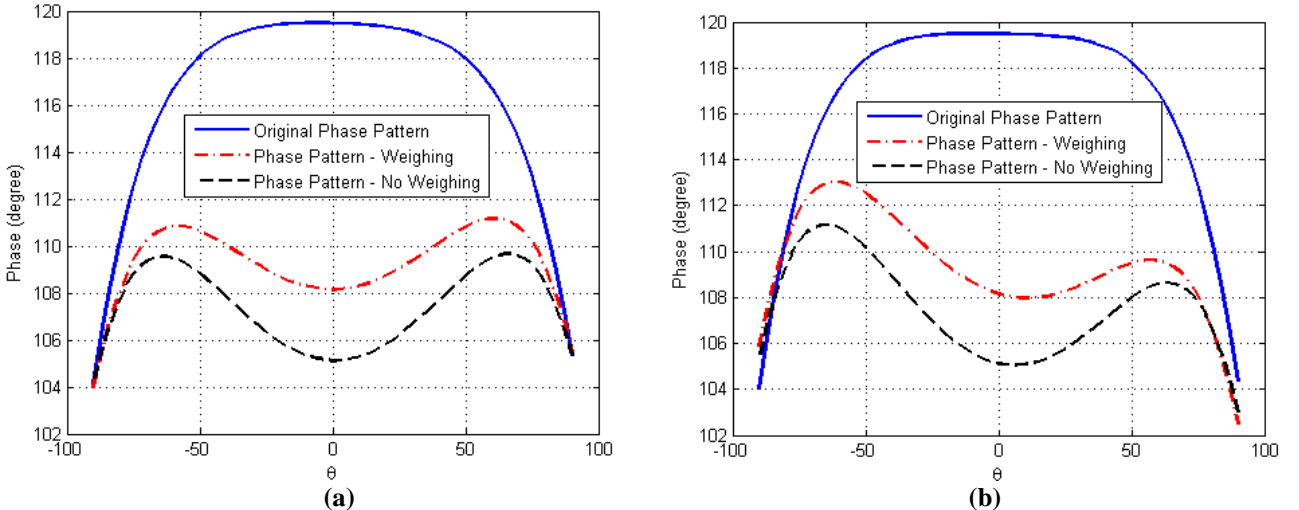


Fig. 3. Comparison of the original phase pattern and the new phase patterns using the power pattern and the uniform distribution ($-90^\circ < \theta < 90^\circ$). (a) $\varphi = 0^\circ$ cut. (b) $\varphi = 90^\circ$ cut.

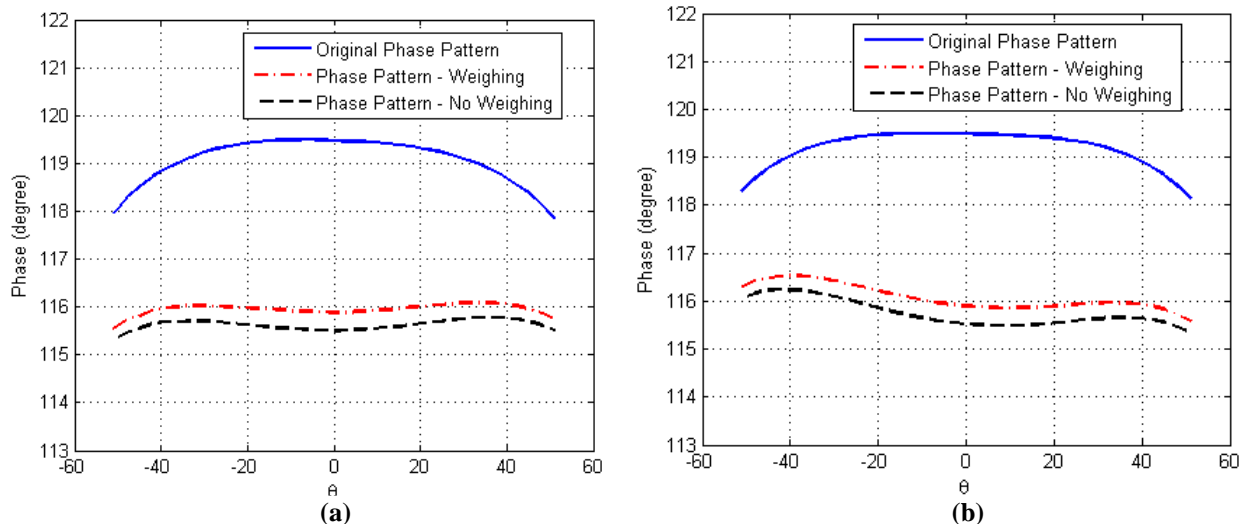


Fig. 4. Comparison of the original phase pattern and the new phase patterns using weightings of the power pattern and the uniform distribution over $(-50^\circ < \theta < 50^\circ)$. (a) $\varphi = 0^\circ$ cut. (b) $\varphi = 90^\circ$ cut.

Table I. Phase Center Positions $(-90^\circ < \theta < 90^\circ)$

Type	Phase Center (mm)	σ^2 (rad^2)
Original	$\mathbf{d} = [0, 0, 0]$	6.710
Non-weighting	$\mathbf{d} = [0, 0.7, 7.6]$	2.109
Weighing	$\mathbf{d} = [-0.1, 1.0, 6.0]$	0.981

Table II. Phase Center Positions $(-50^\circ < \theta < 50^\circ)$

Type	Phase Center (mm)	σ^2 (rad^2)
Original	$\mathbf{d} = [0, 0, 0]$	0.087
Non-weighting	$\mathbf{d} = [-0.1, 0.2, 2.1]$	0.005
Weighing	$\mathbf{d} = [-0.1, 0.2, 1.9]$	0.003

4. Conclusion

A method for determining the three-dimensional phase center of an antenna is presented. The new phase pattern with respect to the origin's spatial displacement \mathbf{d} (Δx , Δy , Δz) can be obtained from the original phase pattern, which corresponds to a phase center at a physical reference position on the antenna. The new phase center is determined by minimizing the variance of the new phase pattern. An exhaustive search is used, but this guarantees a best solution to attain the accuracy of the test volume, and the computation time is just minutes on a standard personal computer. The technique is illustrated for a GPS antenna using different examples of angular weighting as probability density functions.

5. References

1. James J. Spilker, *Global positioning system: theory and applications*, Progress in astronautics and aeronautics, 1996.
2. P. Miller, M. Alexander and Tian Hong Loh, "Antenna phase center determination in the presence of phase errors," *Antennas and Propagation, EuCAP2009.*, pp. 1978-1982, March 2009.
3. A. Prata, "Misaligned Antenna Phase-Center Determination Using Measured Phase Patterns," *The Interplanetary Network Progress Report*, IPN PR 42-150, pp. 1-9, April-June 2002.
4. P. Padilla, et al., "Experimental Determination of DRW Antenna Phase Center at mm-Wavelengths Using a Planar Scanner: Comparison of Different Methods," *IEEE Transactions on Antennas and Propagation*, vol. 59, issue 8, pp. 2806-2812, Aug. 2011.
5. Jun-ping Shang, et al., "Measurement of phase center for antenna with the method of moving reference point," *Antennas, Propagation and EM Theory, 2008. ISAPE 2008. 8th International Symposium on*, pp. 114 -117, Nov. 2008.
6. Pieter N. Betjes, "An Algorithm for Automated Phase Center Determination and its Implementation," *Nearfield Systems, Inc.*, the Netherlands, 2007.
7. Warren L. Stutzman, *Polarization in Electromagnetic Systems*, Artech House, Boston. 1992.